Supporting Information

Facile Fabrication of Hollow CuO Nanocubes for Enhanced Lithium/Sodium Storage Performance

Jie Zhao,[a,b] Yuyan Zhao,[c] Wen-Ce Yue,[a,d] Shu-Min Zheng,[a] Xue Li,[a] Ning Gao,[a,b] Ting Zhu,*[e] Yu-Jiao Zhang,*[a] Guang-Ming Xia,[d] and Bao Wang,*[a,b]

a. State Key Laboratory of Biochemical Engineering, Institute of Process Engineering, Chinese Academy of Sciences, Beijing 100190, China.

b. Nanjing IPE Institute of Green Manufacturing Industry, Nanjing 211135, China.

c. Key Laboratory of Bio-inspired Materials and Interfacial Science, Technical Institute of Physics and Chemistry, Chinese Academy of Sciences, Beijing, 100190, China.

d. School of Chemistry and Chemical Engineering, University of Jinan, Jinan 250022, China.

e. School of Materials Science & Engineering, Central South University, Changsha, Hunan 410083, China

* Corresponding author: E-mails: baowang@ipe.ac.cn; ZYJ_20170112@163.com; zhut0002@csu.edu.cn

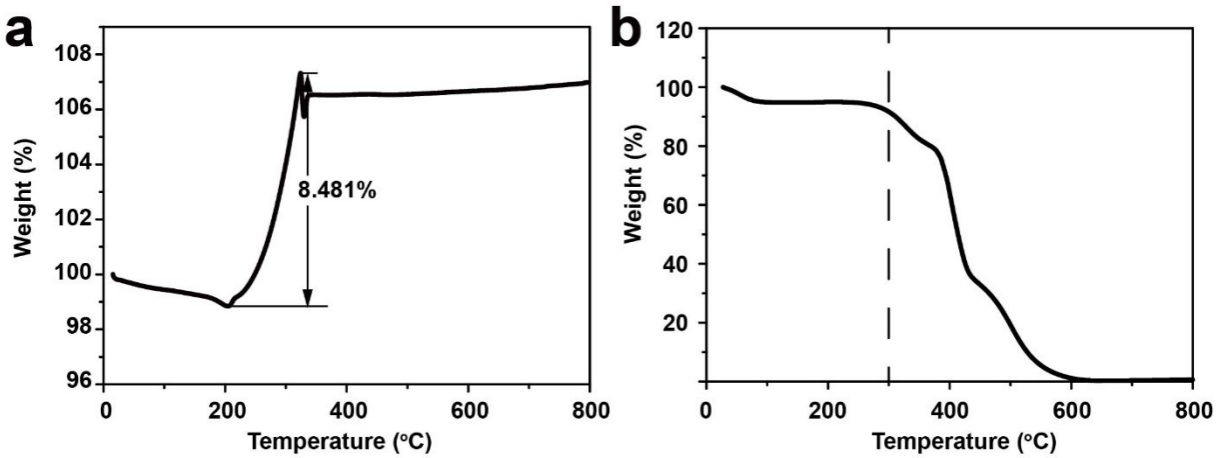

Fig. S1 Thermogravimetric curve of (a) Cu_2O nanocubes and (b) PVP.

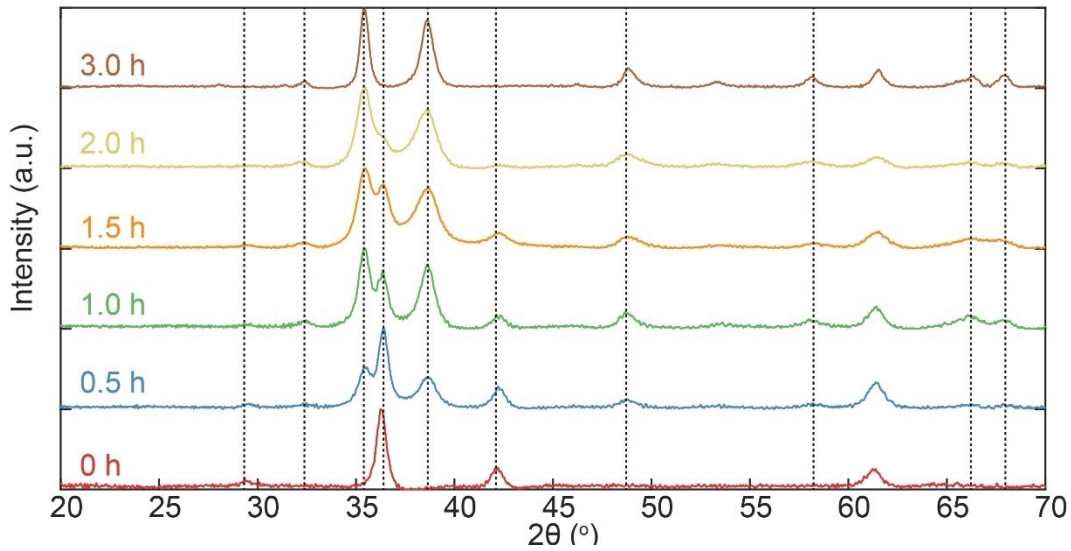

Fig. S2 XRD spectra of Cu_2O nanocubes after varying time in-air heating.

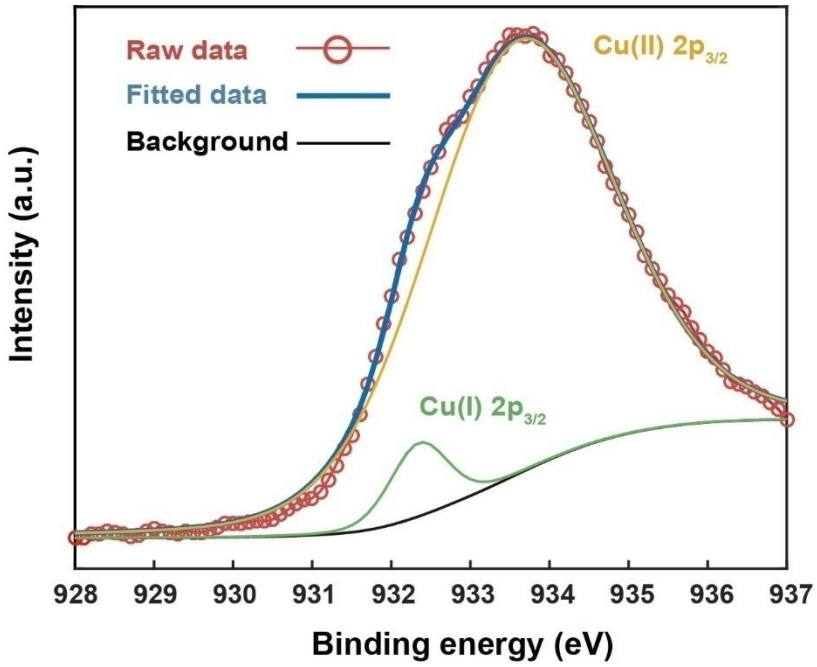

Fig. S3 XPS peaks of Cu $2p_{3/2}$ for the insufficiently transformed CuO nanocubes.

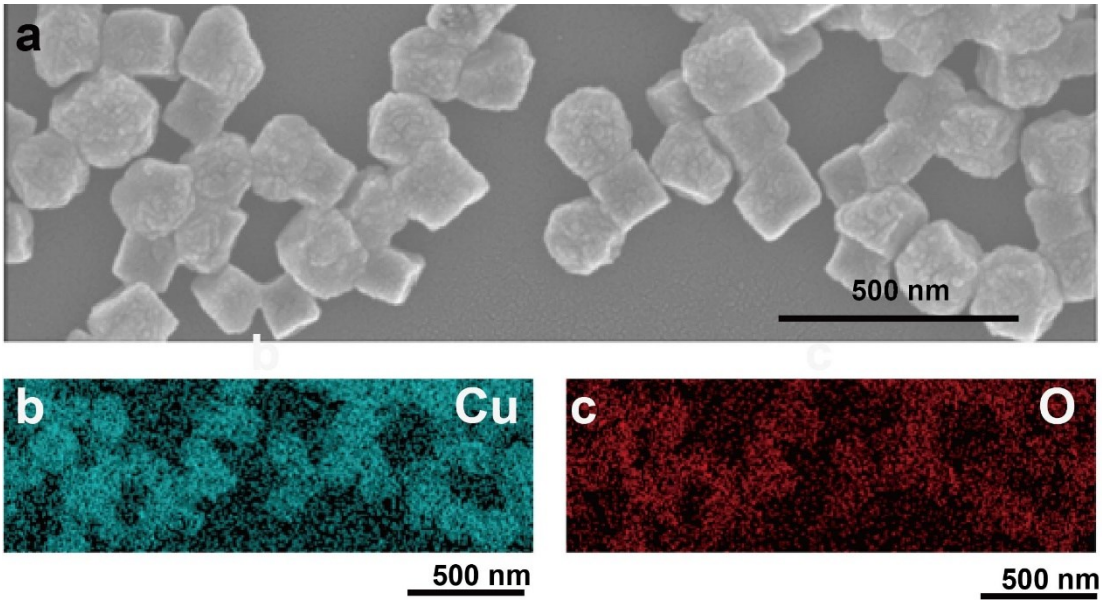

Fig. S4 SEM image and corresponding elemental mapping analysis of CuO nanocubes.

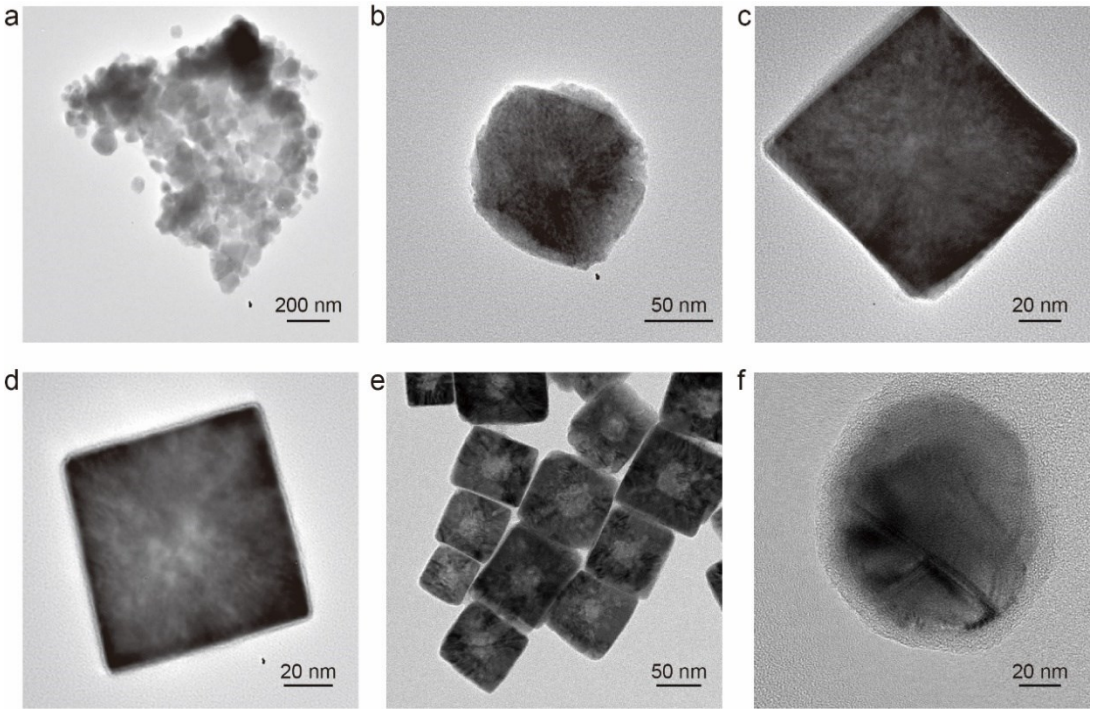

Fig. S5 SEM images of the sample in solvothermal process with a) 3 h, b) 6 h, c) 9 h, d) 12, e) 24 h, and f) 48 h.

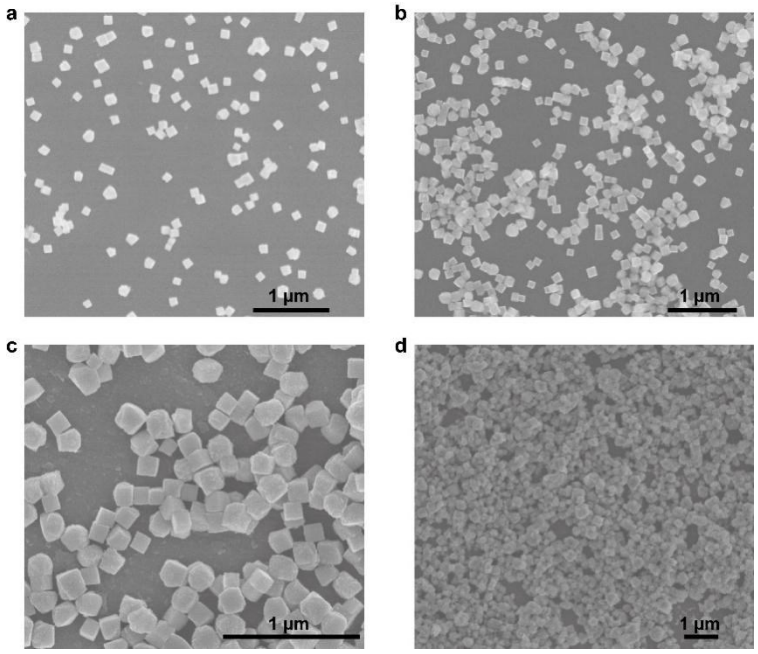

Fig. S6 SEM images of the Cu_2O nanocubes with (a)100 mg, (b), 200 mg, (c) 500 mg, and (d) 1000 mg of $Cu(acac)_2$ utilized in solvothermal reaction.

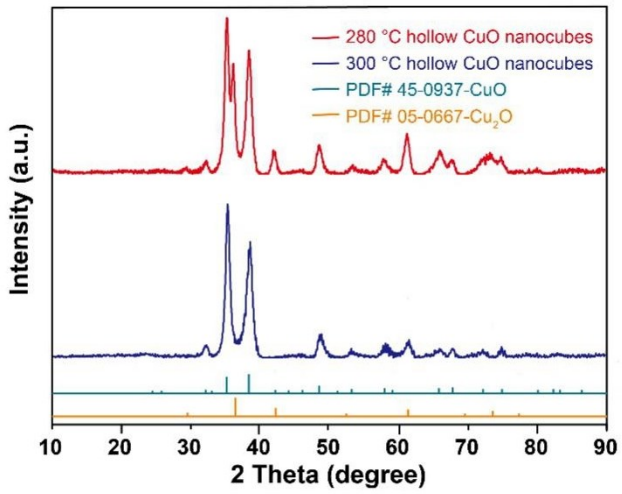

Fig. S7 XRD of the CuO nanocubes after in-air annealing at 280 °C and 300 °C.

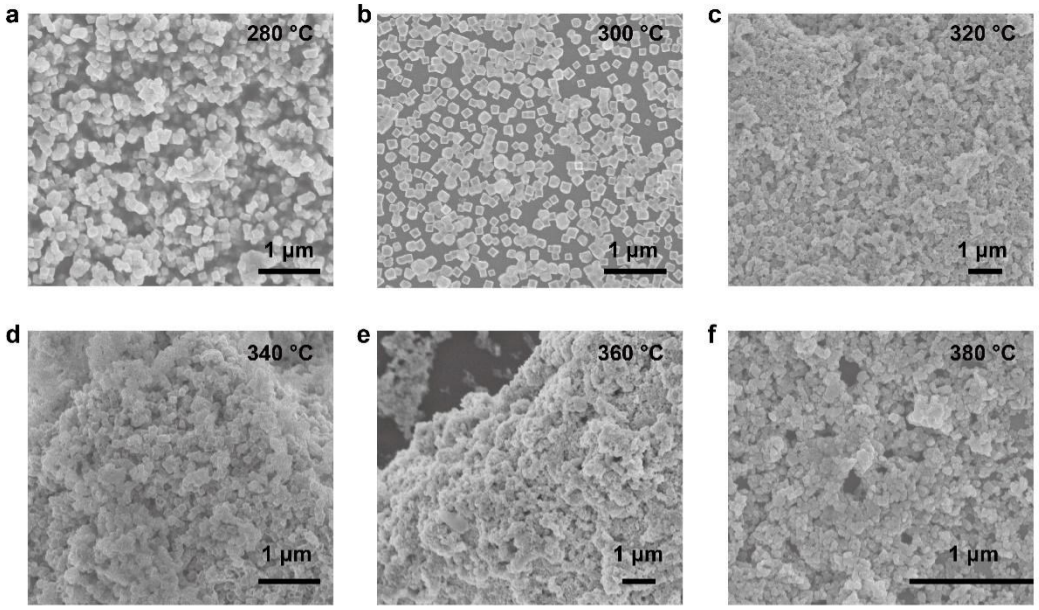

Fig. S8 SEM images of the CuO nanocubes after in-air annealing at various temperatures. In-air annealing was conducted at (a) 280 °C, (b) 300 °C, (c) 320 °C, (d) 340 °C, (e) 360 °C and (f) 380 °C.

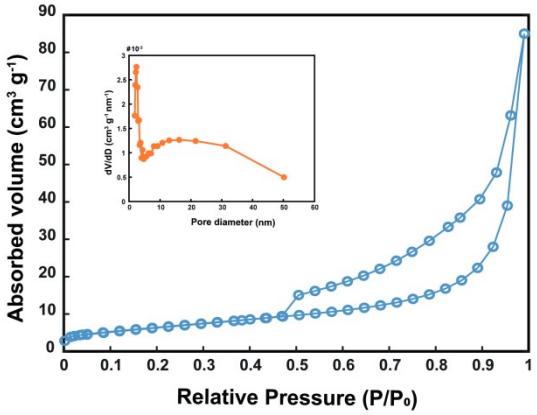

Fig. S9 N_2 adsorption/desorption isotherms of CuO hollow nanocubes. Inset showed pore size distribution of CuO hollow nanocubes.

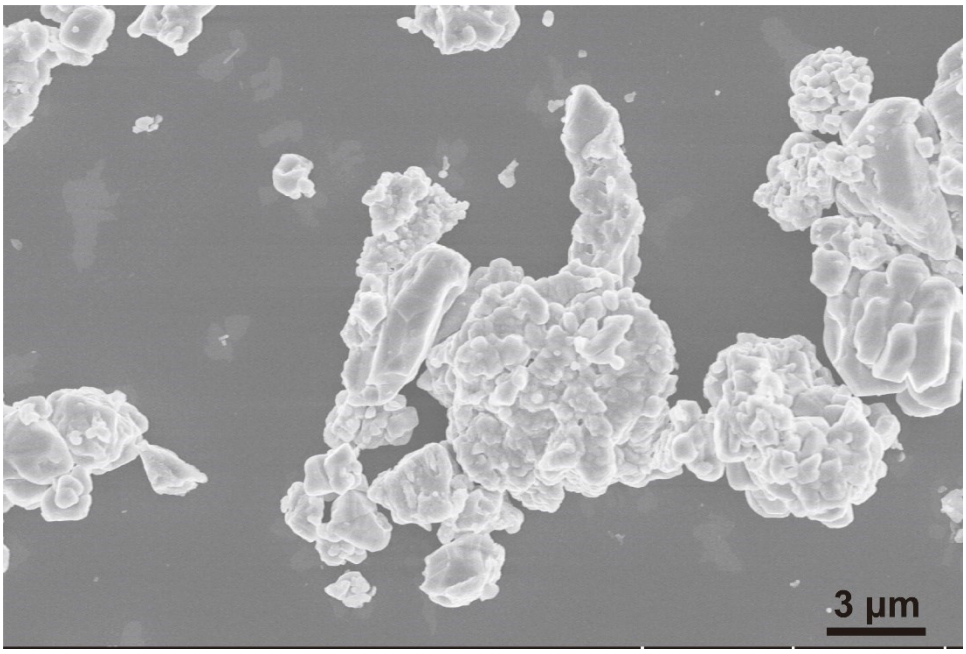

Fig. S10 SEM image of commercialized CuO micro/nanoparticles.

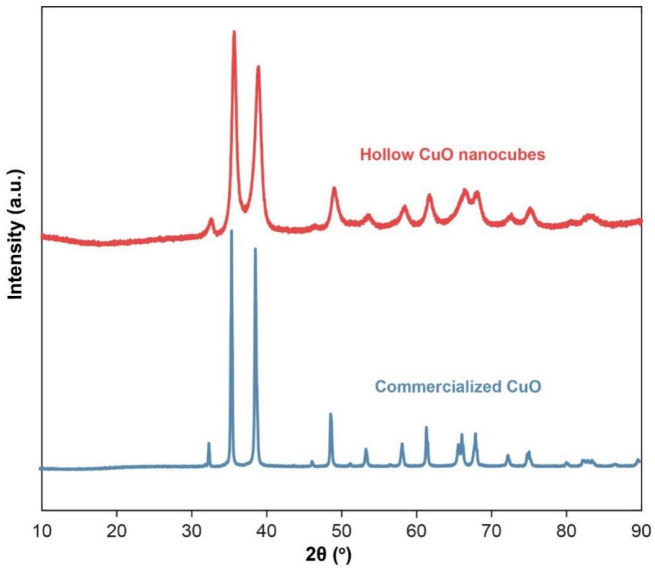

Fig. S11 XRD spectra of hollow CuO nanocubes and commercialized CuO nanocubes.

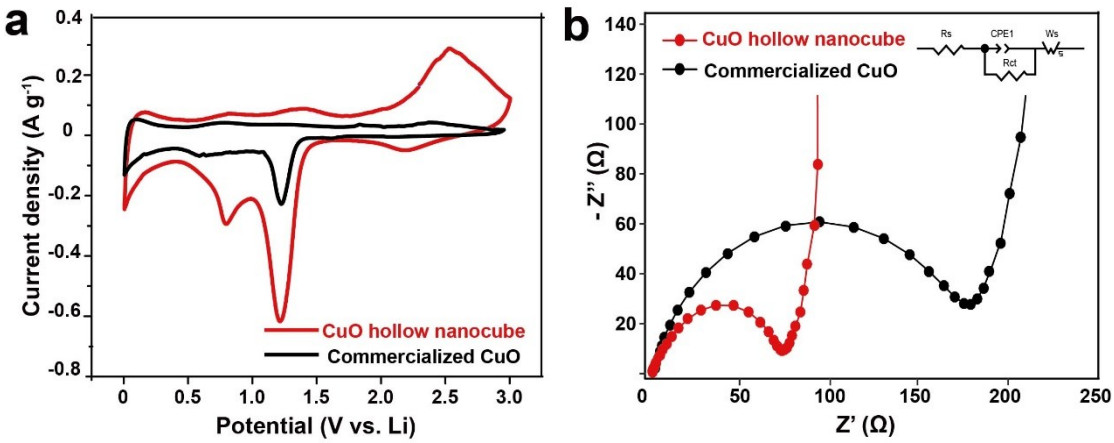

Fig. S12 (a) Comparison of CV curves of hollow CuO nanocubes and commercialized CuO electrodes at a scan rate of 0.1 mV s^{-1}; (b) Electrochemical impedance spectra of CuO electrodes.

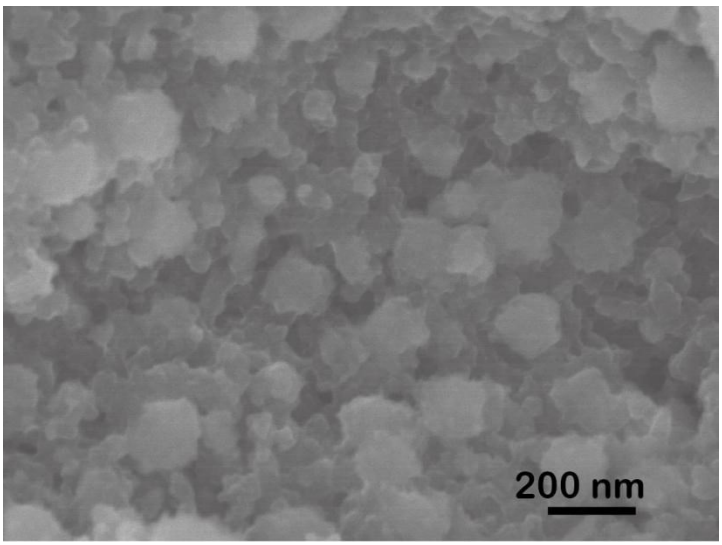

Fig. S13 SEM image of hollow CuO nanocubes after 100 cycles.

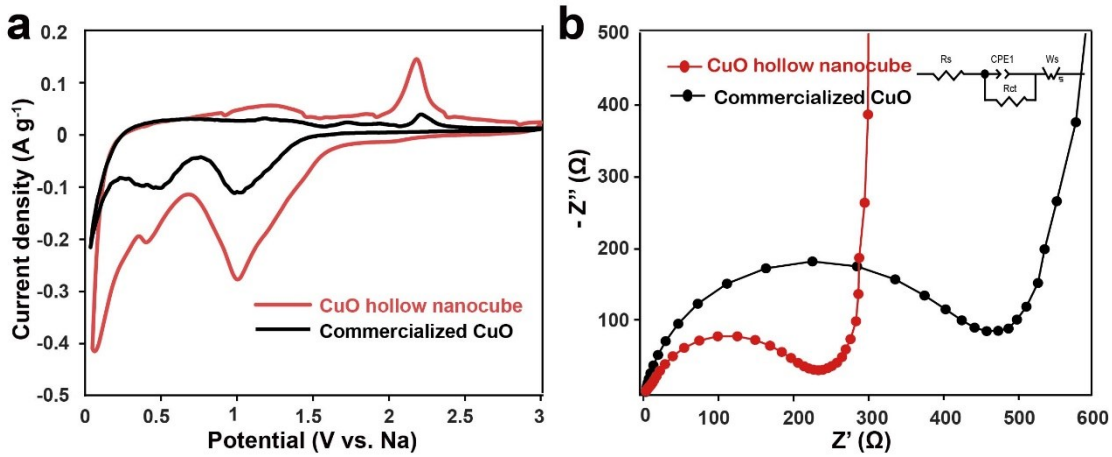

Figure S14. (a) Comparison of CV curves of hollow CuO nanocubes and commercialized CuO electrodes at a scan rate of 0.1 mV s^{-1}. (b) Electrochemical impedance spectra of CuO electrodes.

Table S1. Comparison of the hollow CuO materials and other transitional oxides materials as anode for LIBs.

Materials	Theoretical capacity（mAh g^{-1})	Current density（ mA g^{-1})	Cycle number	Specific Capacity (mAh g^{-1})	Ref.
CuO hollow nanotubes	674	100	160	552	[1]
CuO microspheres	674	0.1 C	50	429.0	[2]
CuO nanoflowers/copper	674	0.5 C	200	486.1	[3]
peony-like CuO	674	0.1 C	200	456	[4]
octahedral CuO	674	0.2 C	50	440	[5]
MnO_2 hollow capsules	1233	50	500	198.4	[6]
NiO hollow spheres	718	100	45	490	[7]
CeO_2 Hollow Nanospheres	623	100	100	639	[8]
MnO nanotubes	756	200	180	680.7	[9]
MnO@C nanorods	756	500	100	186.3	[10]
Hollow NiO nanotubes	718	200	100	620	[11]
hollow CoO	715.4	120	55	589.1	[12]
Hollow CuO nanocubes	674	100	100	865	This work

Table S2. Comparison of the hollow CuO materials and other transitional oxides materials as anodes for SIBs.

Materials	Theoretical capacity（m Ah g^{-1})	Current density (mA g^{-1})	Cycle number	Specific capacity (mAh g^{-1})	Ref.
Flower-like carbon-coated CuO	674	500	100	189	[13]
N-doped carbon coated CuO array	674	500	100	214.97	[14]
CuO nanosheets.	674	500	40	218	[15]
Nanoporous CuO/Cu composites	674	500	100	200	[16]
TiO_2/carbon hollow spheres	335	500	100	97	[17]
bowl-like hollow Co_3O_4	890	200	10	290	[18]
Hollow CuO nanocubes	674	500	100	216	This work

References

1 C. Kong, W. Lu, J. Zong, F. Pu, X. Hu, X. Zhang, Z. Yang, F. Wang and H. Jin, Template-assisted synthesis of CuO hollow nanotubes constructed by ultrathin nanosheets for lithium-ion battery applications, *J. Alloys Compd.*, 2020, **849**, 156635.

2 C. Wang, D. Higgins, F. Wang, D. Li, R. Liu, G. Xia, N. Li, Q. Li, H. Xu and G. Wu, Controlled synthesis of micro/nanostructured CuO anodes for lithium-ion batteries, *Nano Energy*, 2014, **9**, 334-344.

3 W. Yuan, Y. Ye, Y. Yang, X. Zhang, B. Pan, Z. Peng, M. Wu, Z. Qiu, C. Wang, Y. Yuan, Z. Yan and Y. Tang, CuO nanoflowers/copper fiber felt integrated porous electrode for lithium-ion batteries, *Sci. China Technol. Sci.*, 2020, **63**, 2423-2434.

4 R. Dang, X. Jia, P. Wang, X. Zhang, D. Wang and G. Wang, Hydrothermal synthesis of peony-like CuO micro/nanostructures for high-performance lithium-ion battery anodes, *Chinese Chem. Lett.*, 2017, **28**, 2263-2268.

5 L. Feng, Z. Xuan, Y. Bai, H. Zhao, L. Li, Y. Chen, X. Yang, C. Su, J. Guo and X. Chen, Preparation of octahedral CuO micro/nanocrystals and electrochemical performance as anode for lithium-ion battery, *J. Alloys Compd.*, 2014, **600**, 162-167.

6 Y. Wang, P.-S. Ding, M.-G. Zou, W.-B. Guo, D.-X. Wang and F.-C. Zhang, Synthesis of nanosheet-based MnO2 hollow capsules and their application in lithium batteries, *Ferroelectrics*, 2018, **522**, 75-79.

7 X. H. Huang, J. P. Tu, C. Q. Zhang and F. Zhou, Hollow microspheres of NiO as anode materials for lithium-ion batteries, *Electrochim. Acta*, 2010, **55**, 8981-8985.

8 M. Sasidharan, N. Gunawardhana, M. Yoshio and K. Nakashima, CeO2 Hollow Nanospheres as Anode Material for Lithium Ion Batteries, *Chem. Lett.*, 2012, **41**, 386-388.

9 S. Zhang, W. He, X. Zhang and X. Yang, Rational design of carbon-coated hollow MnO nanotubes for Li-ion batteries, *J. Mate. Sci.Mater. Electron.*, 2015, **26**, 2189-2197.

10 X. Zhang, G. Zhu, D. Yan, T. Lu and L. Pan, MnO@C nanorods derived from metal-organic frameworks as anode for superiorly stable and long-life sodium-ion batteries, *J. Alloys Compd.*, 2017, **710**, 575-580.

11 L. Liu, Y. Guo, Y. Wang, X. Yang, S. Wang and H. Guo, Hollow NiO nanotubes synthesized by bio-templates as the high performance anode materials of lithium-ion batteries, *Electrochim. Acta*, 2013, **114**, 42-47.

12 Y. Li, Q. Guan, J. Cheng, W. Ni and B. Wang, Carbon-coated hollow CoO microporous nanospheres synthesized by CoF2 as the intermediates as anode materials for lithium-ion batteries, *Ionics*, 2018, **24**, 1587-1594.
13 S. Xu, L. Lu, Q. Zhang, Q. Jiang, Z. Luo, S. Wang, G. Li and C. Feng, A Facile Synthesis of Flower-Like CuO as Anode Materials for Lithium (Sodium) Ion Battery Applications, *J. Nanosci. Nanotechno.*, 2016, **16**, 7655-7661.
14 Y. Li, M. Zhang, J. Qian, Y. Ma, Y. Li, W. Li, F. Wang, L. Li, F. Wu and R. Chen, Freestanding N‐Doped Carbon Coated CuO Array Anode for Lithium‐Ion and Sodium‐Ion Batteries, *Energy Technol.*, 2019, **7**.
15 Y. Liu, Y. Qiao, W. Zhang, P. Hu, C. Chen, Z. Li, L. Yuan, X. Hu and Y. Huang, Facile fabrication of CuO nanosheets on Cu substrate as anode materials for electrochemical energy storage, *J. Alloys Compd.*, 2014, **586**, 208-215.
16 T. Zheng, G. Li, D. Li and X. Meng, Based on Cu as framework constructed nanoporous CuO/Cu composites by a dealloy method for sodium-ion battery anode, *J. Nanopart Res.*, 2018, **20**.
17 F. Yang, Z. Zhang, Y. Han, K. Du, Y. Lai and J. Li, TiO_2 /carbon hollow spheres as anode materials for advanced sodium ion batteries, *Electrochim. Acta*, 2015, **178**, 871-876.
18 J.-W. Wen, D.-W. Zhang, Y. Zang, X. Sun, B. Cheng, C.-X. Ding, Y. Yu and C.-H. Chen, Li and Na storage behavior of bowl-like hollow Co3O4 microspheres as an anode material for lithium-ion and sodium-ion batteries, *Electrochim. Acta*, 2014, **132**, 193-199.